1-8-2011

Screening of siRNA Nanoparticles for Delivery to Airway Epithelial Cells Using High Content Analysis

Alan Hibbitts
Royal College of Surgeons in Ireland

Nora Lieggi
University College Dublin

Olive McCabe
Royal College of Surgeons in Ireland

Warren Thomas
Royal College of Surgeons in Ireland

James Barlow
Royal College of Surgeons in Ireland

See next page for additional authors

Citation

Hibbitts A, Lieggi N, McCabe O, Thomas W, Barlow J, O'Brien F, Cryan SA. Screening of siRNA Nanoparticles for Delivery to Airway Epithelial Cells Using High Content Analysis. Therapeutic Delivery. 2011;2(8):987-999.

Authors
Alan Hibbitts, Nora Lieggi, Olive McCabe, Warren Thomas, James Barlow, Fiona O'Brien, and Sally-Ann Cryan

Screening of siRNA Nanoparticles for Delivery to Airway Epithelial Cells Using High Content Analysis

Alan Hibbitts[1], Nora Lieggi[2], Olive McCabe[3], Warren Thomas[3], James Barlow[1, 4], Fiona O'Brien[1], Sally-Ann Cryan[1*]

[1] School of Pharmacy, Royal College of Surgeons in Ireland, Dublin 2, Ireland

[2] Veterinary Science Centre, University College Dublin, Belfield, Dublin 4, Ireland

[3] Department of Molecular Medicine, Education and Research Centre, Beaumont Hospital, Dublin 9, Ireland

[4] Department of Pharmaceutical & Medicinal Chemistry, Royal College of Surgeons in Ireland, Dublin 2, Ireland

*For Correspondence

Sally-Ann Cryan BSc (Pharm), PhD

School of Pharmacy

York House, York Street

Royal College of Surgeons in Ireland

Dublin 2

Tel: +353-14022741 Fax: +353-14022765

email:scryan@rcsi.ie

Abstract

- **Background**

Delivery of siRNA to the lungs via inhalation offers a unique opportunity to develop novel methods of treating a range of poorly treated respiratory conditions. However progress has been greatly hindered by safety and delivery issues. This study developed a high-throughput method for screening novel nanotechnologies for pulmonary siRNA delivery

- **Methodology**

Following physico-chemical analysis, the ability of PEI-PEG/siRNA nanoparticles to facilitate siRNA delivery was determined using high content analysis (HCA) in Calu-3 cells. Results obtained from HCA were validated using confocal microscopy. Finally, cytotoxicity of the PEI-PEG/siRNA particles was analysed by HCA using the Cellomics® multiparamter cytotoxicity assay.

- **Conclusions**

PEI-PEG/siRNA nanoparticles facilitated increased siRNA uptake and luciferase knockdown in Calu-3 cells compared to PEI/siRNA.

Defined Key Terms:

High Content Analysis

High content analysis is a high throughput screening method which involves a computational approach to the characterization of the functions of specific target proteins and other cellular constituents, along with whole-cell functions. This primarily achieved by employing fluorescence cell-based assays and microscopy

RNAi

RNA interference (RNAi) is an endogenous system in eukaryotic cells by which sequence-specific RNAs are able to bind and degrade its complementary mRNA thereby halting protein expression[1]

PEI

Polyethylenimine (PEI) polymers are a synthetic polymer group with an amine group at every 3rd atom. They have been found to possess a good ability to complex DNA and RNA and transiently transfect cells. However, PEI has been noted to exert a cytotoxic effect which has been found to be proportional to its molecular weight [2].

Mitochondrial Membrane Potential

A loss in Mitochondrial Membrane Potential (MMP) has been shown to result in the induction of apoptosis through a number of channels. These include (i) disruption of electron transport, oxidative phosphorylation, and adenosine triphosphate (ATP) production; (ii) release of proteins that trigger activation of caspase family proteases (i.e. Ctytochrome C); and (iii) alteration of cellular reduction-oxidation (redox) potential [3].

Cytochrome C

Cytochrome C (Cyt-C) is an essential component of the mitochondrial respiratory chain. It is a soluble protein that is localized in the intermembrane space and is loosely attached to the surface of the inner mitochondrial membrane. Cytosolic Cyc forms an essential part of the vertebrate “apoptosome,” which is composed of Cyc, Apaf-1, and procaspase-9. The result is activation of caspase-9, which then processes and activates other caspases to orchestrate the biochemical execution of cells [4]

1. Introduction

From preliminary investigations, it has become apparent that systemic naked short interfering RNA (siRNA) treatment has a low therapeutic potential. This is primarily related to the rapid excretion and degradation of siRNA and poor intracellular trafficking. Naked siRNA has a half life of less than one hour in human plasma and circulating siRNA is rapidly excreted by kidneys due to its small size [5]. In addition, naked siRNA is unable to cross the lipid membrane of a cell due to its size and negative charge. This then leads to insufficient tissue bioavailability. These issues are also compounded by non-specific cellular uptake [5-7] and the cytotoxicity on systemic administration via interferon activation through toll-like receptor 7 (TRL-7) [8].

In contrast, local delivery of siRNA to the lungs offers several important benefits including reduced dosing and a reduction in side effects due to local targeted delivery. Lastly, and most importantly in the context of treating respiratory disease, local delivery of siRNA allows direct access to lung epithelial cells, an important cell type in a variety of pulmonary disorders. Among the myriad of lung pathologies in which epithelial cells are thought to play an important role are diseases such as cystic fibrosis, chronic obstructive pulmonary disease, asthma, and pulmonary fibrosis [9].

Unfortunately, the lung possesses a number of both physical and immunologic barriers that can hinder the effectiveness of aerosolised nanoparticles [10, 11]. These barriers include degradation in the cytoplasm coupled with rapid clearance via muco-cilliary activity and toxicity concerns [12]. Aerosolised nanoparticles are being

explored as a non-viral means of delivering siRNA to the lungs. Polymers including PEI are used to complex siRNA and protect them from degradation during biophysical aerosolisation in vivo. Large, time consuming screens are required for screening novel biomaterials and nanotechnologies for intracellular delivery and toxicity testing. Current methods including confocal microscopy and spectrofluorometry are both time and resource consuming. The development of high content analysis (HCA) platforms has made great progress in addressing this issue. Herein, we propose HCA as a high throughput method for analysing nanoparticle interaction with cells, specifically airway cells. HCA technology relies upon the integration and automation of quantitative fluorescence microscopy and image analysis to yield a high volume of both quantitative and qualitative information. Having evolved over the last decade [13], HCA is dived into two discreet stages. The first consists of fluorescence microscopy and cell staining using a range of fluorescence-based reagents. These allow for specific intracellular organelles and signalling molecules to be tagged and visualised. Following on from this, data acquisition is then undertaken using image analysis software (In Cell® 1000 Workstation software in the case of this paper). The analysis algorithms available therein then allow for a cell-specific level of data analysis over numerous different parameters. HCA has been used successfully in the analysis of a number of different processes such as intracellular trafficking, cell signalling pathways and cytotoxicity [14-17]. Furthermore, the use of HCA for cytotoxicity studies has been validated for specificity and sensitivity using multi-target analysis for hundreds of marketed drugs [18].

Complexation with poly(ethylene imine) (PEI) has long been established as a means of effectively delivering nucleic acids to pulmonary cells due to its ability to be effectively released from the endosome using the "proton sponge" effect [19]. However, there have also been long standing concerns over its toxicological profile and an its inability to overcome the mucous barrier of the lung [12, 20]. The addition of poly(ethylene glycol) (PEG) appears to overcome a number these hurdles by creating muco-inert particles with improved toxicity profiles and enhanced intracellular trafficking. With particular regard to the lung, PEG-modified particles have been found to successfully overcome the endogenous mucus of the pulmonary epithelium [21-23]. It is hypothesised that the use of a novel PEI-PEG construct combining the high level of transfection associated with PEI with the biocompatibility and improved trafficking of PEG will lead to effective siRNA therapy in the lungs.

In this study, HCA was harnessed to assess the ability of nanoparticles composed of PEI and PEI-PEG for delivery of siRNA to airway epithelial cells. HCA was used to examine the ability of different polymer-siRNA combinations to be internalized by human bronchial (Calu-3) epithelial cells at a wide range of doses. Calu-3 cells are derived from a bronchial adenocarcinoma in a 25 year old Caucasian male and are a well known model cell line[24]. These cells have been documented as presenting with a fully differentiated apical epithelial with maximum trans-epithelial resistance (TER) following 11+ days of culture in an air/liquid interface. Furthermore, after screening for ultrastructure, levels of airway secretory proteins and mRNA, Calu-3 cells exhibit the mRNA and protein content characteristic of the native epithelium[25]. When cultured at an air-liquid interface, they form mucus producing, well differentiated and polarised monolayers with tight junctions that generate significant transepithelial electrical resistance[26].

Evidence of internalisation in Calu-3 cells was then cross-referenced with in vitro genetic knockdown and confocal microscopy studies. Cytotoxicity induced by the nanoparticles was also determined using HCA together with the Cellomics® Multiparameter Cytotoxicity 3 kit. That allows a comprehensive screen of nuclear intensity (NI), nuclear area (NA), cytochrome-c levels (Cyt-C), mitochondrial membrane potential (MMP), plasma membrane permeability (PMP) and cell number (CN).

2. Experimental

Materials

All cell culture and HCA reagents were obtained from Invitrogen Corporation (CA, USA), unless otherwise stated. The Calu-3 bronchial epithelial cell line was obtained from the American Tissue Type Culture Collection (ATCC) and used at passages 20-50. All poly(ethylene glycol) molecules were obtained from Iris Biotech (Marktredwitz, Germany). siGENOME Non-Targeting siRNA #2 and #4 and ON-TARGETplus GAPD Control (5' UAAGGCUAUGAAGAGAUAC 3' and 5' AUGAACGUGAAUUGCUCAA 3' and 5' GUCAACGGAUUUGGUCGUA 3' respectively) were obtained from Dharmacon (USA). The non-targeting sequences are non-specific for human gene sequences and specific for firefly luciferase using the Promega pGL3 cloning vector. All other general chemicals and reagents used were of the highest grade possible and were obtained from Sigma-Aldrich Company Ltd. (Dorset, UK), unless otherwise stated.

PEI-PEG Synthesis

PEI-PEG polymers were synthesised by reaction of succinimidyl-activated PEG (PEG-SSA) with PEI under slightly basic aqueous conditions as previously described [19]. Briefly, 1g of 25 kDa PEI was dissolved in 25 mL of phosphate buffered saline (pH 8). Following this, 500 mg of a known molecular weight PEG-SSA was dissolved in 5 mL of 99.9% dimethyl sulfoxide (DMSO). This was added drop-wise, with stirring, to the PEI solution in the required stoichiometric ratio (Table 1). The reaction was allowed to proceed for 4 hours at room temperature before being stopped by the addition of 60mL of deionised water. The reaction mixture was transferred to Cellu•Sep H1 membranes (25kDa MWCO) (Orange Scientific) and dialysed overnight in excess deionised water to remove unreacted components. The dialysate was replaced with fresh deionised water for a further 4 hours, and repeated a total of 4 times before being lyophilised. Final products were then analysed for form and purity using ^{1}H and ^{13}C NMR spectroscopy (Bruker), FT-IR (Bruker) spectroscopy, gel permeation chromatography (GPC) (Perkin Elmer) and electronic light scattering detection (Polymer Labs).

Plasmid Preparation

pGL3-Control Vector plasmid (Promega) consists of 5256bp and contains the firefly luciferase gene and an ampicillin resistance gene that are controlled by a SV40 promotor/enhancer. The plasmids were replicated in the high-copy DH5-α *Escherichia coli* strain grown in selective ampicillin (50 μg/mL) supplemented Luria-Bertani medium, isolated by alkaline lysis followed by anion exchange

chromatography using the Giga Qiagen kit (Qiagen, UK) according to the manufacturer's protocol. Purity of the plasmid and integrity of the cDNA insert were determined by agarose gel electrophoresis and UV spectroscopy (E 260/280 nm ratio). After isolation, the DNA was dissolved to an end concentration of 1.2 μg/μL TrisHCl buffer (pH 8.0). The purity of the plasmid was assayed by 1% agarose gel electrophoresis.

PEI-PEG/siRNA Nanoparticle Formation and Characterisation

Polymer-siRNA complexes were formed using a variety of PEI nitrogen to RNA phosphate (N/P) ratios ranging from 1-10. Briefly, the appropriate amount of polymer was added to an siRNA solution (20μM) to yield a final concentration of 2μM siRNA, vortexed for 10 s and incubated for polyplex formation for 30 min. Particle size and ζ-potential were determined using a nano-ZS (Malvern). Size and ζ-potential analysis programmes consisted of 5 separate scans which contained 15 sub-scans.

High Content Analysis Screening of Nanoparticle Uptake into Calu-3 Cells

Calu-3 cells were seeded at $3x10^4$ cells/well in a 96-well plate (Nunc). Nanoparticles were formed as previously described and cells were treated in 150μL serum-free Dulbecco's modified Eagle's medium (DMEM) using 130 nM fluorescently tagged FITC-siRNA. Following 2 hours incubation at 37^oC and 5% CO_2, cells were washed with PBS and fixed using 4% paraformaldehyde. Cells were stained using phalloidin-TRITC and Hoechst nuclear stain. Image analysis was achieved using the InCell® 1000 High Content Analyzer (GE Healthcare, UK). Four random fields were viewed

per well and the various N/P ratios were repeated in triplicate. Fluorescence intensity of the dyes was monitored at the excitation and emission wavelengths specific to each dye. (i.e. 360 nm and 460 nm for Hoechst, 480 nm and 535 nm for FITC-siRNA and 535 nm and 600 nm for phalloidin-TRITC). Exposure times were varied to optimise image quality. However, typical exposure and hardware autofocus (HWAF) values were: (1) 100 ms and 11.1 µm for Hoechst 33342; (2) 250 ms and − 1.1 µm for FITC-siRNA and (3) 300 ms and − 2.1 µm for phalloidin-TRITC. After acquisition of the images, the data was analysed using In Cell® 1000 Workstation software (GE Healthcare, UK) using multi-target analysis with a variety of settings for each of the parameters (Table 2). All samples were run in triplicate and the experiment repeated on 3 independent occasions.

Laser Scanning Confocal Microscopy (CLSM) Analysis of Nanoparticle Uptake and Intracellular Trafficking into Calu-3 cells

Calu-3 cells were seeded at $1x10^5$ cells/well on sterile acid washed coverslips in a 24-well plate. Nanocomplexes were formed as previously described with the optimum N/P ratios as determined by HCA analysis for each polymer selected for analysis using 200nM of FITC-siRNA. Cells were treated with the complexes under the same conditions as in HCA screening and fixed to glass slides prior to analysis using the LSM510 confocal microscope and Zeiss LSM imaging software.

To assess the intracellular trafficking of the polymer-siRNA nanocomplexes following internalisation cells were seeded and transfected as above. Cells were then incubated for 4 hours before counterstaining. Lysosomes were stained using

LysoTracker® Red DND-99 (LTR) (Invitrogen) and nuclei were stained with Hoechst 33342 using methods modified from previously described methods [27, 28]. Briefly, treated cells were washed and then stained with 100μL of 200nM LTR for 20min at 37 °C. Following dye uptake, LTR was removed and slides were rinsed twice with 200μL of warm PBS before fixing with 4% paraformaldehyde for 20min at RT. Cells were rinsed again with PBS and stained with 200μL of Hoechst 33342 diluted in 400μL of PBS for 5min at RT protected from the light. Cells were then fixed to glass slides prior to analysis using the LSM510 confocal microscope and Zeiss LSM imaging software.

Luciferase siRNA Knockdown in Calu-3 Cells

For luciferase knockdown experiments, cells were seeded at a density of $5x10^4$ in 48-well plates 24hrs prior to transfection. Following this, cells were first transfected with luciferase control vector plasmid and SuperFect® transfection reagent (Qiagen, UK). Cells were transfected using 0.75μg of pDNA/3μL of SuperFect in 100μL serum-free DMEM per well for 4 hours. Cells were then washed 3 times with warm PBS and transfected with anti-luciferase siRNA-polymer complexes (formed as previously described) at 100nM/well in 250μL of serum-containing media and incubated for 24 hours at 37^oC and 5% CO_2. Luciferase expression was assessed using the luciferase assay system (Promega) and read using a Wallac 1420 Multilabel Counter (Perkin Elmer). Protein expression in each sample was examined using the Micro BCA™ protein assay kit (Pierce). All samples were run in quadruplicate and the experiment repeated on 3 independent occasions.

Real Time PCR Analysis of Glyceraldehyde-3-phosphate dehydrogenase *(*GAPDH*)* Knockdown in Fully Differentiated Calu-3 Cells

Calu-3 cells were seeded in Transwell® permeable chambers at $5x10^5$ cells/well. Cells were then cultured in complete media in both apical and basal sides for 1 week and for a further 12 days at an air/liquid interface. On the day of transfection, cells were transfected with 800nM ON-TARGETplus GAPD Control siRNA for 24hrs using preprepared nanocomplexes. Following this, media and transfection complexes were removed and the cells were rinsed twice with warm PBS prior to RNA extraction.

RNA was extracted using the RNeasy Micro Kit (Qiagen, UK) following the manufacturer's instructions. cDNA for real-time PCR was synthesised from RNA using the high capacity reverse transcription kit (Applied Bio-systems, USA) according to the manufacturer's instructions. Quantitative PCR was performed in 200 µl tubes using a Rotor-gene 6000 (Corbett Research, UK) thermal cycler with real-time detection of fluorescence. PCR was conducted in a volume of 25 µl using Rotor-Gene SYBR Green RT-PCR kit (Qiagen, UK). PCR consisted of an initial activation step at 95^{o}C for 5 min followed by cycles of denaturation for 5 s at 95^{o}C, annealing for 10 s at 60^{o}C and melt step for 10 min. The fluorescence intensity of SYBR green I was read and acquired at 60^{o}C after completion of the extension step of each cycle.

Percentage knockdown of GAPDH was then quantified using the dComparative QuantitationT software supplied by Corbett Research for the Rotorgene. The mean efficiency of a group of cycling curves is calculated at the point that the cycling curves take off and used to calculate a fold change according to the formula: fold

change=efficiency Ct1–Ct2, where Ct1 and Ct2 are the take off values of the cycling curves being compared. In all experiments human β-actin was used as a housekeeping gene for comparison of RNA extraction efficiency and knockdown specificity. All samples were run in triplicate and the experiment repeated on 3 independent occasions.

HCA Screening of NanoParticle Induced Toxicity

24 hours prior to transfection, cells were seeded $3x10^4$/well in a 96-well plate. Polymer-siRNA complexes were formed as previously described and cells were treated with 100nM siRNA for 24 hours. Furthermore selected wells were treated with 120μM valinomycin for 24 hours as a positive control prior to analysis. Following incubation, cells were stained and fixed using the Cellomics® Multiparameter Cytotoxicity 3 kit (Thermo Scientific) according to its protocol. Briefly, cells were live stained for mitochondrial membrane potential and plasma membrane permeability. Cells were then fixed using 4% paraformaldehyde before staining with Hoechst nuclear stain and fluorescent antibody labelling for cytochrome-c. Image acquisition was determined using the InCell® 1000 High Content Analyzer.

Four random fields were viewed per well and the various N/P ratios were repeated in quadruplicate. Fluorescence intensity of the dyes was monitored at the excitation and emission wavelengths specific to each dye. (i.e. 360 nm and 460 nm for Hoechst, 480 nm and 535 nm for the permeability dye, 535 nm and 600 nm for mitochondrial membrane potential dye and 646/674 nm for DyLight 649 conjugates).

Exposure times were varied between experiments to optimise image quality. However, typical exposure and hardware autofocus (HWAF) values were: (1) 40-75 ms and 0-11.1 µm for Hoechst; (2) 100-200 ms and − 1.1-5 µm for the PMP dye; (3) 150-200 ms and − 2.1-0 µm for the MMP dye; and (4) 150-200 ms and − 0.6-0 µm for the DyLight 649 conjugates. Following acquisition of the images, the data was analysed using In Cell® 1000 Workstation software (GE Healthcare, UK) using multi-target analysis with a variety of settings for each of the parameters (Table 3). All samples were run in quadruplicate and the experiment repeated on 3 independent occasions

Statistical Analysis

Data returned was treated as parametric and statistical analysis was carried out against controls using the Students t-test. A $p<0.05$ was taken to be statistically significant.

3. Results & Discussion

PEG Grafting to PEI

The PEI-PEG grafting reaction based on the succinimdyl-modified PEG was chosen as an efficient method of achieving high yields of modified polymers using a minimum of reaction steps [29]. Using this one step method, it appears that PEI-PEG grafting was successfully achieved in all reactions. Evidence of this was found in the ^{13}C NMR due to the presence of amide bonds between the amine group of PEI and the succinimdyl group of the PEG. The level of grafting for each molecular weight of

PEG was determined through the integration of the PEG and PEI signals in the ^{1}H NMR. GPC analysis of the polymers also demonstrated an increased molecular weight consistent with polymer formation as well as a high level of purity. For the polymers used in this study there was a minimum of 60% PEG grafting to PEI in all cases as demonstrated in Table.1.

PEI-PEG/siRNA Nanocomplex Size and Zeta Potential

At comparable N/P ratios, PEI-PEG copolymers formed significantly ($P<0.001$) more compact particles than unmodified PEI-siRNA as demonstrated by a general decrease in particle size (Figure1). ζ-potential analysis also demonstrated that PEI-PEG polymers formed cationic nanocomplexes with siRNA at lower N/P ratios in comparison to unmodified PEI (Figure1 B). While it has been well documented that PEI is adept at efficiently encapsulating both plasmid DNA (pDNA) and siRNA [30, 31], it has also become apparent that PEGylation of PEI can have a positive effect on encapsulation. Specifically, Mao *et al.* demonstrated the effect that varying the molecular weight and grafting density of PEG can result in PEI-PEG-siRNA nanoparticles smaller than their corresponding unmodified PEI-siRNA nanoparticles at the same N/P ratio [32]. Furthermore, it has also been found that higher molecular weight PEGs can induce nucleic acid condensation in their own right [33]. Owing to the highly PEGylated nature of the polymers used in this study, it is reasonable to assume that the addition of PEG molecules is playing a positive role in siRNA encapsulation.

HCA Analysis of Nanoparticle Uptake into Calu-3 Cells

Using HCA analysis, the effect of N/P ratio on PEI-PEG/siRNA was determined and compared to RNAiFECT and siRNA alone (Figure 2). It was found that at higher N/P ratios the PEI(25kDa)-PEG(10kDa)/siRNA nanoparticles exhibited the highest overall level of uptake of all nanoparticles. At higher N/P ratios, there was a large difference between the uptake seen in the PEI-PEG(10kDa)/siRNA nanoparticles compared to PEI alone and PEI-PEG(5kDa). In contrast, the unmodified PEI(25kDa) and PEI(25kDa)-PEG(5kDa)/siRNA nanoparticles both exhibited relatively poor levels of siRNA uptake. It is thought that this is increase in uptake efficiency with increasing N/P ratio is primarily due to the high level of PEGylation reducing non-specific interactions between the nanoparticle and the cell and improving endocytosis [34, 35].

Confocal Microscopy Analysis of Nanoparticle Uptake into Calu-3 cells

To validate the HCA, additional images were taken using traditional confocal microscopy techniques. These studies confirmed that PEI-PEG/siRNA nanopartciles were successfully internalised into the Calu-3 cells (Figure3 A+B). Furthermore, on analysis of the lysotracker red (LTR) staining it was found that both internalised PEI-PEG(5kDa)/(10kDa)/siRNA nanoparticles co-localised with LTR stained vacuoles (Fig.3 C+D). Lysotracker Red DND-99 is a cationic fluorescent dye that preferentially accumulates in the acidic lysosomal compartments of cells [27]. Therefore, co-localisation of the FITC-siRNA and LTR can be taken as an indication that the siRNA nanoparticles have been successfully internalised into the cell prior to escape and subsequent genetic knockdown. This lends support to ny assumptions

made from the images taken from the HCA regarding the internalisation of administered nanoparticles.

Luciferase Knockdown by siRNA Nanoparticles in Calu-3 cells

To assess the optimal nanoparticle composition for siRNA knockdown Calu-3 cells were transfected with a luciferase plasmid using a commercial reagent and then treated PEI/PEI-PEG nanoparticles at a range of N/P ratios (1-10). PEI-PEG/siRNA nanoparticles had the ability to mediate significant siRNA knockdown of luciferase expression ($P<0.05$) (Figure4). PEI-PEG(10kDa)/ siRNA nanoparticles were capable of knocking down expression by over 50% ($P<0.05$) at N/P=10. Critically, the trend for increase in knockdown observed for these nanoparticles at higher N/P ratios was broadly in line with the levels of uptake first observed in HCA nanoparticle uptake analysis (Figure. 2). PEI-PEG(5kDa)-siRNA particles were also capable of increased levels of genetic knockdown at all N/P ratios. At an N/P ratio=7, the percentage knockdown rivalled knockdown efficacy observed in the PEI-PEG(10kDa) samples. However, the decrease at higher N/P ratios could relate cytotoxic effects. In comparison, unmodified PEI-siRNA nanoparticles exhibited relatively poor levels of genetic knockdown. Furthermore, genetic knockdown was also only seen at the highest 3 N/P ratios. From these results it is hypothesised that the high level of PEGylation present in both polymers may have resulted in an increase in overall transport of siRNA nanoparticles[22]. This is especially true when the size and zeta potentials of each nanoparticles are taken into consideration. Since at comparable sizes and zeta potentials at the higher N/P ratios, the PEGylated polymers retain a distinct increase in abilty to effect genetic knockdown.

Real Time PCR Analysis of GAPDH Knockdown in Fully Differentiated Calu-3 Cells

To determine the ability of the nanoparticles to overcome the mucous barrier a fully differentiated cell model was required. On examination of GAPDH knockdown, it was found that results were also representative of the screening information previously seen in the HCA analysis of polymer-siRNA uptake. The overall percentage of cells transfected was low; this necessitated the use of additional higher N/P ratios than previously used in undifferentiated knockdown experiments. This clearly demonstrated the well known difficulty in transfecting differentiated cells related to both the non-dividing nature of the cells and the presence of a mucous barrier. PEGylated polymers showed increased uptake over unmodified-PEI/siRNA nanocomplexes. In particular, the PEI-PEG(10kDa)-siRNA nanoparticles demonstrated a noticeable increase in knockdown efficiency in comparison to PEI/siRNA nanoparticles (47±4% in PEI-PEG(10kDa) at N/P=15 compared with 14%±15.5% in unmodified PEI at N/P=15). These results are in line with recently published data which documented the increased ability of PEG coated polystyrene particles to overcome the difficulties presented by mucosal membranes [22]. These studies involving mucous producing fully differentiated Calu-3 cells are the first to clearly indicate that PEI-PEG had a superior ability to deliver siRNA and effect knockdown compared with umodified PEI-siRNA nanoparticles.

Cellomics® Screening of Cytotoxicity in Calu-3 Cells

Overall, it was found that all nanoparticles were well tolerated over the useful dose ranges (Figure5) with all nanoparticles exhibiting cytotoxicity at higher N/P ratios (Figure6+7). This was determined through the combined examination of each of the 6 parameters measured. Analysis of cell number (CN) (Figure.5a) was determined by counting the number of specific cell nuclei per well as a means of assessing cell growth and population number. It was found that PEI-PEG(10kDa)-siRNA nanocomplex treated wells had an approximately 20% increase in cell number in comparison to untreated wells at all dose levels used for transfections. Similarly, unmodified PEI-siRNA nanocomplexes also exhibited a tendency to be well tolerated by Calu-3 cells, however, PEI samples did not exhibit the levels of cell proliferation observed in the PEGylated samples. Further to this, PEI-siRNA nanoparticles actually demonstrated a decrease in cell numbers across all N/P ratios. These results would be in line with recent findings indicating the toxic nature of PEI and the pro-inflammatory nature of PEI-PEG [23]

Evidence of this cell proliferation was also seen in the nuclear morphology analysis of treated cells. Nuclear morphology can be taken as an indication of cell health via analysis of nuclear staining intensity and nuclear area. Nuclei of cells undergoing apoptosis are known to contract in size as their chromatin condenses, this in turn leads to a greater level of intensity when stained using Hoechst. On examination, it was

found that all nanoparticles did not exhibit any significant changes in nuclear intensity (NI) (Figure. 5b) of cells at therapeutic N/P ratios. This would indicate that at no point is there evidence of the chromatin condensation associated with cell death. However in the case of PEI-PEG(5kDa) and PEI-PEG(10kDa) treated cells chromatin condensation was significantly increased at higher N/P doses which corresponded to the observed decrease in cell population. On analysis of nuclear area (NA) (Figure. 5c), there was less evidence of cytotoxicity with no statistically significant changes observed in the positive control. However there was a signifigant drop in nuclear area in the PEI-siRNA treated sample, although without a significant drop in NA observed in the controls it is difficult to make any definte conclusions.

For further analysis of cytotoxicity, samples were also examined for mitochondrial membrane potential (MMP), plasma membrane permeability (PMP) and cytochrome-c (Cyt C).

As stated in the key terms, loss of MMP is followed by cell death through the release of Cyt-C and the triggering of numerous other signalling pathways. On MMP analysis (Figure. 5d), PEI-PEG(10kDa)-siRNA showed no significant difference from untreated cells whereas at higher N/P ratios all nanoparticles demonstrated an increase in MMP similar to that seen in the valinomycin treated samples. (This increase may be seen as the beginning of a MMP spike before a drop off in MMP levels as seen in other studies [17]).

On examination of Cyt C levels (Figure. 5e), valinomycin treated cells were found to induce a large increase of Cyt C in Calu-3 cells. In comparison, PEI-PEG(5kDa) and

PEI-PEG(10kDa)-siRNA treated cells exhibited the lowest level of change from control followed PEI-siRNA. Both of these polymers resulted in relatively lower levels of Cyt C at low N/P ratios and an increase in Cyt C at higher N/P ratios with PEI-PEG(10kDa) treated cells beginning to decrease in Cyc at N/P=50. Again, this may be evidence of a cell-injury related spike in Cyt C levels before a large drop off indicating cell death. However, the lack of change in Cyt-C levels prior to this (especially with regard to the changes observed in the valinomycin controls) would preclude this as a viable hypothesis.

A reduction in PMP following cellular insult has been shown to occur in pre-apoptotic cells in tandem with mitochondrial membrane destabilisation [36]. Analysis of all nanoparticles at higher N/P ratios (Figure. 5f) demonstrated the beginning of nuclear localisation of the PMP (as a result of nuclear membrane breakdown). In comparison, the remaining polymer-siRNA conjugates remained constant or below that of the control samples. This overall decrease in other samples was seen to be as a result of the continued proliferation of their cells. The increase in cell number would also result in a dilution effect in staining since the amount of dye available per cell would decrease resulting in a drop in fluorescence intensity. Furthermore, the increased amount of tight junctions present in a confluent/semi-confluent Calu-3 population would present an additional barrier to dye penetration.

In vivo studies to date involving PEI and its derivatives and siRNA delivery have previously shown that local delivery of siRNA to the lung is possible [37]. Previous research has demonstrated that cytotoxicity and biological activity in PEGylated PEI is dependent on both the level of PEGylation of the polymer and the molecular weight

of the PEG in question [23, 32]. Encouraging results have been encountered regarding both the production of genetic knockdown and the investigation of resulting toxicity of PEI-based nanoparticles [37, 38]. These studies have shown that while PEGylation has the desired effect of reducing toxicity, the issue of the proinflammatory effects of the delivered particles remains a concern for future clinical applications. In contrast unmodified PEI was shown to have a low inflammatory effect but had a higher level of cytotoxicity. However the signalling pathways and triggering mechanisms for these processes remain poorly characterised. It is our belief that with the additional level of detail obtained through the use of the Cellomics® multiparameter toxicity and novel HCA methods a clearer picture of the mechanisms involved in cytotoxicity and the point at which it occurs has been achieved.

4. Conclusions

The application of HCA is well established for "hit" screening of lead, active compounds for pharmaceutical research. However, it has yet to be properly harnessed for the screening the cell-interaction and toxicity of biomaterials and drug delivery systems. Using the InCell® 1000 and the appropriate software, we were able to rapidly screen a range of polymeric-siRNA nanoparticles and identify the most efficient polymer and nanoparticle composition for siRNA delivery to airway cells. By determining the most efficient nanoparticle composition with the least cytotoxicity we were able to establish an overall lead nanotechnology for further in vivo studies.

The key finding of this screen was that PEGylated PEI particularly PEI-PEG(10kDa) facilitated significantly more siRNA airway cell uptake than unmodified PEI. This

resulted in improved knockdown of reporter gene luciferase by PEI-PEG(10kDa), significantly greater than the knockdown mediated by the control PEI samples.

Finally, multiparameter cytotoxicity screening carried out using HCA indicated that PEGylation of PEI with 10kDa PEG led to a reduction in cytotoxicity even at high N/P ratios PEI:siRNA compared to unmodified PEI. Finally, the PEI-PEG (10kDa) was capable of forming a "muco-inert" siRNA nanoparticle capable of delivering siRNA across a mucous layer and into differentiated cells, thereby offering an innovative siRNA nanotechnology suitable for local targeting to the airway cells after inhalation.

5. Future Perspectives

PEI-PEG(10kDa):siRNA nanotechnology can overcome the mucous barrier, effect knockdown >50% and is biocompatible and therefore offers a unique siRNA delivery platform. To date, there have been preclinical trials involving *in vivo* delivery of modified PEI to the lungs [37] and PEI-PEG(10kDa):siRNA nanotechnology will now be screened *in vivo* for siRNA delivery. By nebulising these nanoparticles the siRNA therapy can be targeted to the lungs for local treatment of respiratory conditions. Aerosolisation of nanoparticles to form nanoaerosols has been facilitated by the development of advanced nebuliser devices including vibrating mesh technologies capable of high efficiency nebulisation [39]. The combination of advances in biomaterials and nanotechnology together with inhaler device design means that nanoaerosol delivery is now more feasible and offers enormous clinical potential. With these technologies a licensed, inhaled siRNA therapy in the next 5-10 years has become a more realistic goal.

The key to this potential however lies in robust and highthroughput screening tools for novel nanotechnologies. HCA based techniques can deliver high volumes of data with minimal biomaterial resources and it is the opinion of this research group that this technology will have become the standard means studying nanotechnologies and nanotoxicology within the next 2-5 years. High content analysis has the potential to play a key role in the development of novel biomaterials for a range of drug delivery and tissue engineering applications, offering a high throughput method for studying biomaterial-cell interaction and toxicity.

High content analysis has the potential to play a key role in the development of novel biomaterials for a range of drug delivery applications including inhalation, offering a high throughput method for studying biomaterial-cell interaction and toxicity including the study of aerosolised nanoparticles and nanotxicology as outlined herein.

6. Executive Summary

- PEI-PEG co-polymers form more compact, cationic nanoparticles at lower N/P ratios than unmodified PEI
- HCA and confocal analysis identified PEI-PEG(10kDa) as the most effective polymer for siRNA delivery to Calu-3 cells, leading to >50% knockdown
- siRNA knockdown facilitated by PEI-PEG(10kDa)/siRNA nanoparticles was superior to gold standard, RNAifect™/PEI.
- PEI-PEG(10kDa)/siRNA nanoparticles were even capable of facilitating siRNA uptake and knockdown of endogenous genes in fully differentiated, mucous covered Calu-3 monolayers,

- HCA screening for toxicity indicated PEI-PEG(10kDa)/siRNA were significantly less toxic than unmodified PEI/siRNA nanoparticles.

7. Acknowledgments

This research was undertaken using generous funding provided by Science Foundation Ireland (SFI) under grant SFI 07/SRC/B1154. Confocal microscopy was provided by The National Biophotonics and Imaging Platform Ireland which was funded by the Higher Education Authority (HEA) through PRTLI 4.

8. References

1. Elbashir Sm, Lendeckel W, Tuschl T: RNA interference is mediated by 21- and 22-nucleotide RNAs. *Genes Dev* 15(2), 188-200 (2001).
2. Godbey Wt, Mikos Ag: Recent progress in gene delivery using non-viral transfer complexes. *J Control Release* 72(1-3), 115-125 (2001).
3. Green Dr, Reed Jc: Mitochondria and apoptosis. *Science* 281(5381), 1309-1312 (1998).
4. Li P, Nijhawan D, Budihardjo I *et al.*: Cytochrome c and dATP-dependent formation of Apaf-1/caspase-9 complex initiates an apoptotic protease cascade. *Cell* 91(4), 479-489 (1997).
5. Li Cx, Parker A, Menocal E, Xiang S, Borodyansky L, Fruehauf Jh: Delivery of RNA interference. *Cell Cycle* 5(18), 2103-2109 (2006).
6. Chiu Yl, Ali A, Chu Cy, Cao H, Rana Tm: Visualizing a correlation between siRNA localization, cellular uptake, and RNAi in living cells. *Chem Biol* 11(8), 1165-1175 (2004).
7. Kim Sh, Mok H, Jeong Jh, Kim Sw, Park Tg: Comparative evaluation of target-specific GFP gene silencing efficiencies for antisense ODN, synthetic siRNA, and siRNA plasmid complexed with PEI-PEG-FOL conjugate. *Bioconjug Chem* 17(1), 241-244 (2006).
8. Hornung V, Guenthner-Biller M, Bourquin C *et al.*: Sequence-specific potent induction of IFN-alpha by short interfering RNA in plasmacytoid dendritic cells through TLR7. *Nat Med* 11(3), 263-270 (2005).
9. De Fougerolles A, Novobrantseva T: siRNA and the lung: research tool or therapeutic drug? *Curr Opin Pharmacol* 8(3), 280-285 (2008).
10. Birchall J: Pulmonary delivery of nucleic acids. *Expert Opin Drug Deliv* 4(6), 575-578 (2007).
11. Weiss Dj: Delivery of DNA to lung airway epithelium. *Methods Mol Biol* 246, 53-68 (2004).

12. Sanders N, Rudolph C, Braeckmans K, De Smedt Sc, Demeester J: Extracellular barriers in respiratory gene therapy. *Adv Drug Deliv Rev* 61(2), 115-127 (2009).
13. Giuliano Ka, Haskins Jr, Taylor Dl: Advances in high content screening for drug discovery. *Assay Drug Dev Technol* 1(4), 565-577 (2003).
14. Bertelsen M, Sanfridson A: Inflammatory pathway analysis using a high content screening platform. *Assay Drug Dev Technol* 3(3), 261-271 (2005).
15. Falschlehner C, Steinbrink S, Erdmann G, Boutros M: High-throughput RNAi screening to dissect cellular pathways: a how-to guide. *Biotechnol J* 5(4), 368-376
16. Grimsey Nl, Narayan Pj, Dragunow M, Glass M: A novel high-throughput assay for the quantitative assessment of receptor trafficking. *Clin Exp Pharmacol Physiol* 35(11), 1377-1382 (2008).
17. Rawlinson La, O'brien Pj, Brayden Dj: High content analysis of cytotoxic effects of pDMAEMA on human intestinal epithelial and monocyte cultures. *J Control Release* 146(1), 84-92
18. O'brien Pj, Irwin W, Diaz D *et al.*: High concordance of drug-induced human hepatotoxicity with in vitro cytotoxicity measured in a novel cell-based model using high content screening. *Arch Toxicol* 80(9), 580-604 (2006).
19. Florea Bi, Meaney C, Junginger He, Borchard G: Transfection efficiency and toxicity of polyethylenimine in differentiated Calu-3 and nondifferentiated COS-1 cell cultures. *AAPS PharmSci* 4(3), E12 (2002).
20. Koping-Hoggard M, Tubulekas I, Guan H *et al.*: Chitosan as a nonviral gene delivery system. Structure-property relationships and characteristics compared with polyethylenimine in vitro and after lung administration in vivo. *Gene Ther* 8(14), 1108-1121 (2001).
21. Suh J, Choy Kl, Lai Sk *et al.*: PEGylation of nanoparticles improves their cytoplasmic transport. *Int J Nanomedicine* 2(4), 735-741 (2007).
22. Tang Bc, Dawson M, Lai Sk *et al.*: Biodegradable polymer nanoparticles that rapidly penetrate the human mucus barrier. *Proc Natl Acad Sci U S A* 106(46), 19268-19273 (2009).
23. Beyerle A, Merkel O, Stoeger T, Kissel T: PEGylation affects cytotoxicity and cell-compatibility of poly(ethylene imine) for lung application: structure-function relationships. *Toxicol Appl Pharmacol* 242(2), 146-154 (2010).
24. Grainger Ci, Greenwell Ll, Lockley Dj, Martin Gp, Forbes B: Culture of Calu-3 cells at the air interface provides a representative model of the airway epithelial barrier. *Pharm Res* 23(7), 1482-1490 (2006).
25. Finkbeiner We, Carrier Sd, Teresi Ce: Reverse transcription-polymerase chain reaction (RT-PCR) phenotypic analysis of cell cultures of human tracheal epithelium, tracheobronchial glands, and lung carcinomas. *Am J Respir Cell Mol Biol* 9(5), 547-556 (1993).
26. Florea Bi, Cassara Ml, Junginger He, Borchard G: Drug transport and metabolism characteristics of the human airway epithelial cell line Calu-3. *J Control Release* 87(1-3), 131-138 (2003).
27. Johnson-Lyles Dn, Peifley K, Lockett S *et al.*: Fullerenol cytotoxicity in kidney cells is associated with cytoskeleton disruption, autophagic vacuole accumulation, and mitochondrial dysfunction. *Toxicol Appl Pharmacol* 248(3), 249-258

28. Rodriguez-Enriquez S, Kim I, Currin Rt, Lemasters Jj: Tracker dyes to probe mitochondrial autophagy (mitophagy) in rat hepatocytes. *Autophagy* 2(1), 39-46 (2006).
29. Lee H, Jeong J, Lee J, Park T: Enhancing Transfection Efficiency Using Polyethylene Glycol Grafted Polyethylenimine and Fusogenic Peptide. *Biotechnology and Bioprocess Engineering* 6(4), 269-273 (2001).
30. Grayson Ac, Doody Am, Putnam D: Biophysical and structural characterization of polyethylenimine-mediated siRNA delivery in vitro. *Pharm Res* 23(8), 1868-1876 (2006).
31. Merkel Om, Librizzi D, Pfestroff A *et al.*: Stability of siRNA polyplexes from poly(ethylenimine) and poly(ethylenimine)-g-poly(ethylene glycol) under in vivo conditions: effects on pharmacokinetics and biodistribution measured by Fluorescence Fluctuation Spectroscopy and Single Photon Emission Computed Tomography (SPECT) imaging. *J Control Release* 138(2), 148-159 (2009).
32. Mao S, Neu M, Germershaus O *et al.*: Influence of polyethylene glycol chain length on the physicochemical and biological properties of poly(ethylene imine)-graft-poly(ethylene glycol) block copolymer/SiRNA polyplexes. *Bioconjug Chem* 17(5), 1209-1218 (2006).
33. Kleideiter G, Nordmeier E: Poly(ethylene glycol)-induced DNA condensation in aqueous/methanol containing low-molecular-weight electrolyte solutionsI. Theoretical considerations. *Polymer* 40(14), 4013-4023 (1999).
34. Petersen H, Fechner Pm, Martin Al *et al.*: Polyethylenimine-graft-poly(ethylene glycol) copolymers: influence of copolymer block structure on DNA complexation and biological activities as gene delivery system. *Bioconjug Chem* 13(4), 845-854 (2002).
35. Gunther M, Lipka J, Malek A, Gutsch D, Kreyling W, Aigner A: Polyethylenimines for RNAi-mediated gene targeting in vivo and siRNA delivery to the lung. *Eur J Pharm Biopharm* 77(3), 438-449
36. Ward Mw, Huber Hj, Weisova P, Dussmann H, Nicholls Dg, Prehn Jh: Mitochondrial and plasma membrane potential of cultured cerebellar neurons during glutamate-induced necrosis, apoptosis, and tolerance. *J Neurosci* 27(31), 8238-8249 (2007).
37. Merkel Om, Beyerle A, Librizzi D *et al.*: Nonviral siRNA delivery to the lung: investigation of PEG-PEI polyplexes and their in vivo performance. *Mol Pharm* 6(4), 1246-1260 (2009).
38. Beyerle A, Braun A, Merkel O, Koch F, Stoeger T, Kissel T: Comparative in vivo study of poly(ethylene imine)/sirna complexes for pulmonary delivery in mice. *J Control Release*,
39. Zhang G, David A, Wiedmann Ts: Performance of the vibrating membrane aerosol generation device: Aeroneb Micropump Nebulizer. *J Aerosol Med* 20(4), 408-416 (2007).

Figure Legends:

Fig.1. (A) Particle size of polymer/siRNA nanoparticles at N/P ratios 1-7 in deionised water. (n=5, *P<0.05 **P<0.001). (B) Zeta potentials of polymer/siRNA complexes at N/P ratios 1-7 in deionised water. (n=5, *P<0.05, **P<0.001). All samples are shown ±SD for both size and zeta potential with significance of PEI-PEG particles measured against values obtained from relative unmodified PEI-siRNA samples.

Fig.2. Quantitative analysis of polymer-siRNA nanoparticle uptake in Calu-3 cells measured using HCA ±SD (n=3 *P<0.05).

Fig.3. Uptake and intracellular trafficking analysis of polymer-siRNA nanocomplexes in Calu-3 cells by LSM510 confocal microscopy (60X). Images were taken approximately 50% through z-stack. (A) PEI-PEG(5kDa)-siRNA N/P=7 , (B) PEI-PEG(10kDa)-siRNA N/P=10 and (C) PEI-siRNA treated cells using 200 nM FITC-labelled siRNA (green) and stained for nuclear body (blue) and cytoplasm (red) or lysosomic vesicles using lysotracker red and co-localisation with FITC-siRNA (yellow, indicated with arrows). (D) PEI-PEG(5kDa)-siRNA N/P=7 , (E) PEI-PEG(10kDa)-siRNA N/P=10 and (F) PEI-siRNA

Fig.4. PEI(-PEG) vs. RNAIFECT-mediated siRNA knockdown of luciferase in Calu-3 cells ±SD (n=3 *P<0.05).

Fig.5. PEI-PEG vs. PEI-mediated siRNA uptake of FITC-siRNA in fully differentiated Calu-3 cells ±SD (n=3 *P<0.05). Significance measured against unmodified PEI-siRNA samples.

Fig.6. Concentration-response curves examining toxic effects of various Polymer-siRNA concentrations on Calu-3 cells after 24 hours. From top, nuclear intensity (NI), nuclear area (NA), cell count (CC), mitochondrial membrane potential (MMP), Cytochrome C (Cyc-C) and plasma membrane permeability (PMP). Readings were compared to 100 % negative controls (* $P < 0.05$, ** $P < 0.01$ compared to controls containing no drug).

Fig.7. Fused images of toxicity in Calu-3 cells. Fused images obtained from analysis consisting of Hoechst nuclear stain (blue), plasma membrane permeability dye (green) and 2^o antibody staining for cytochrome c (red). (A) untransfected control cells, (B) valinomycin treated cells, (C) PEI-PEG(5kDa) N/P=10, (D) PEI-PEG(10kDa) N/P=10, (E) PEI-PEG(5kDa) N/P=50 and (F) PEI-PEG(10kDa) N/P=50

Fig.8. 20x image of Calu-3 cells stained using the Cellomics® Multiparamter Cytotoxicity kit. Fused images obtained from analysis consisting of Hoechst nuclear stain (blue), plasma membrane permeability dye (green) and 2^o antibody staining for cytochrome c (red). (A) Untransfected control (B) Valinomycin treated cells

Tables:

Table.1. Composition of PEI-PEG conjugation experiments using the Succinimidyl Succinate PEG method

Mw PEG (kDa)	PEI used (µmol)	PEG used (µmol)	Stoichiometry (PEI:PEG)	%Yield	Grafting (PEI:PEG)
5 (linear)	40	100	1:2.5	76	1:0.6
10 (linear)	40	50	1:1.25	70	1:0.8

Table.2. Settings for In Cell® 1000 Workstation analysis of Polymer-siRNA nanoparticle uptake into Calu-3 cells

Feature	Source	Segmentation	Min. Area	Sensitivity	Collar
Nuclei	Wave 1 (Hoechst)	Top Hat	50µm^2	100%	
Cell	Wave 2 (TRITC)	Collar	-	-	8µm
Organelles	Wave 3 (FITC)	Cytoplasm only	0.05-0.5µm	3	-

Table.3. Settings for In Cell® 1000 Workstation analysis of Polymer-siRNA nanoparticle induced toxicity in Calu-3 cells

Feature	Source	Segmentation	Min. Area	Sensitivity	Collar
Nuclei	Wave 1 (NA, NI, CN)	Top Hat	50µm^2	100%	-
Cell	Wave 2 (PMP)	Collar	-	-	8µm
Reference 1	Wave 3 (Cyt-C)	Pseudo-Cells	-	-	-
Reference 2	Wave 4 (MMP)	Pseudo-Cells	-	-	-
Reference 3	Wave 2 (PMP)	Pseudo-Nuclei	-	-	-

Figures:

Fig.1.

A.

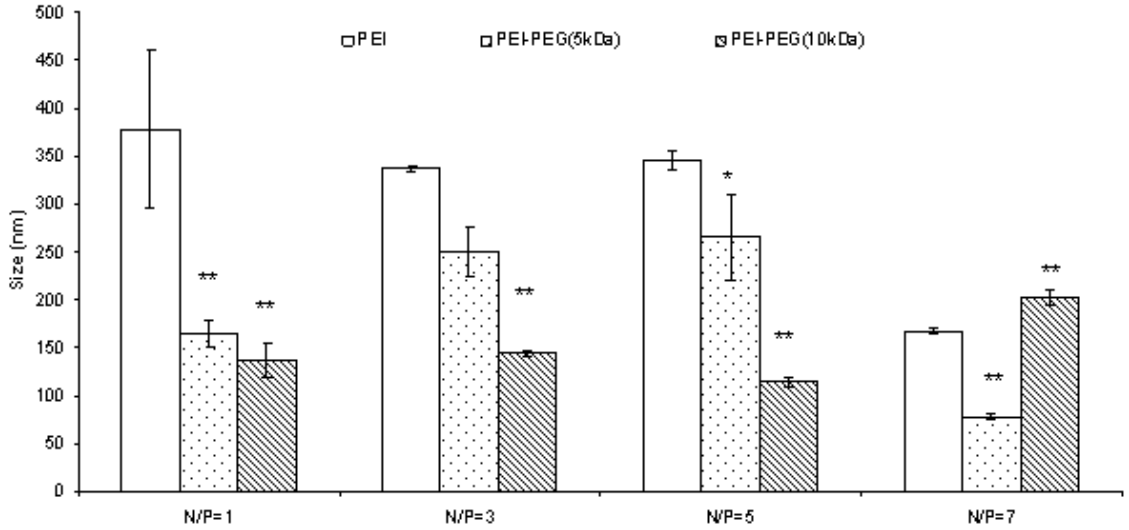

B.

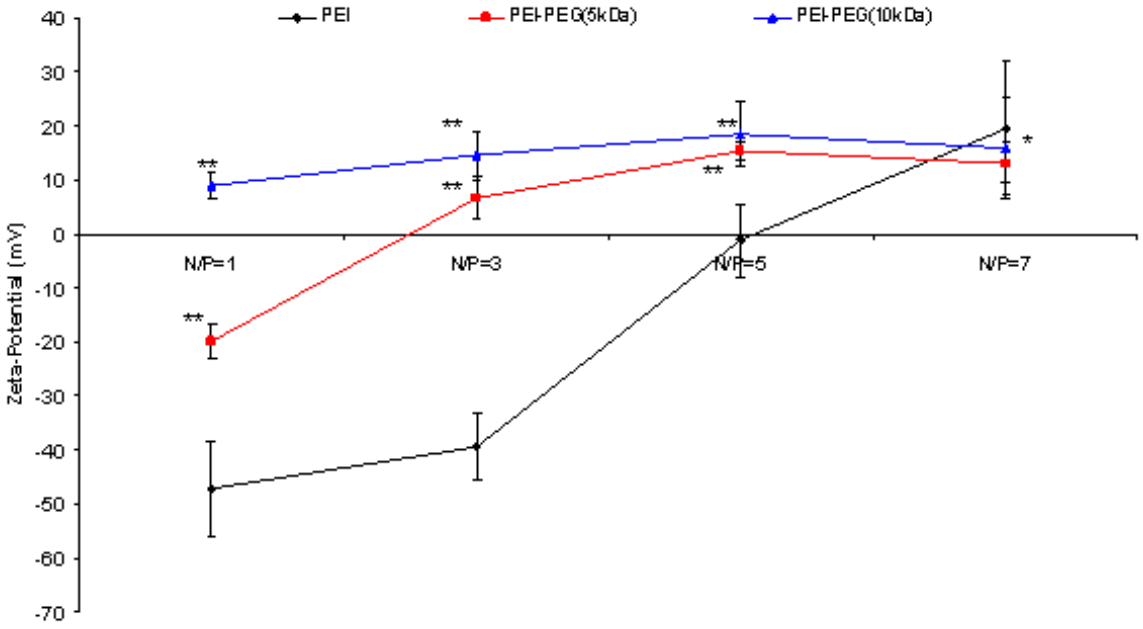

Fig.2.

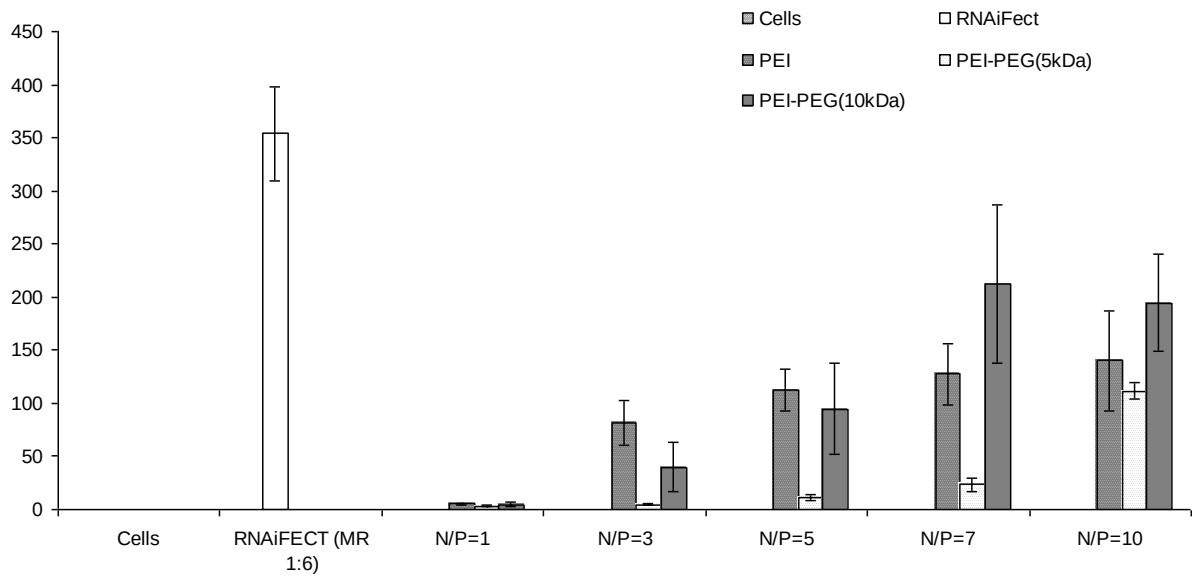
Cells
RNAiFect
PEI
PEI-PEG(5kDa)
PEI-PEG(10kDa)
450
400
350
300
250
200
150
100
50
0
Cells
RNAiFECT (MR 1:6)
N/P=1
N/P=3
N/P=5
N/P=7
N/P=10

Fig.3.

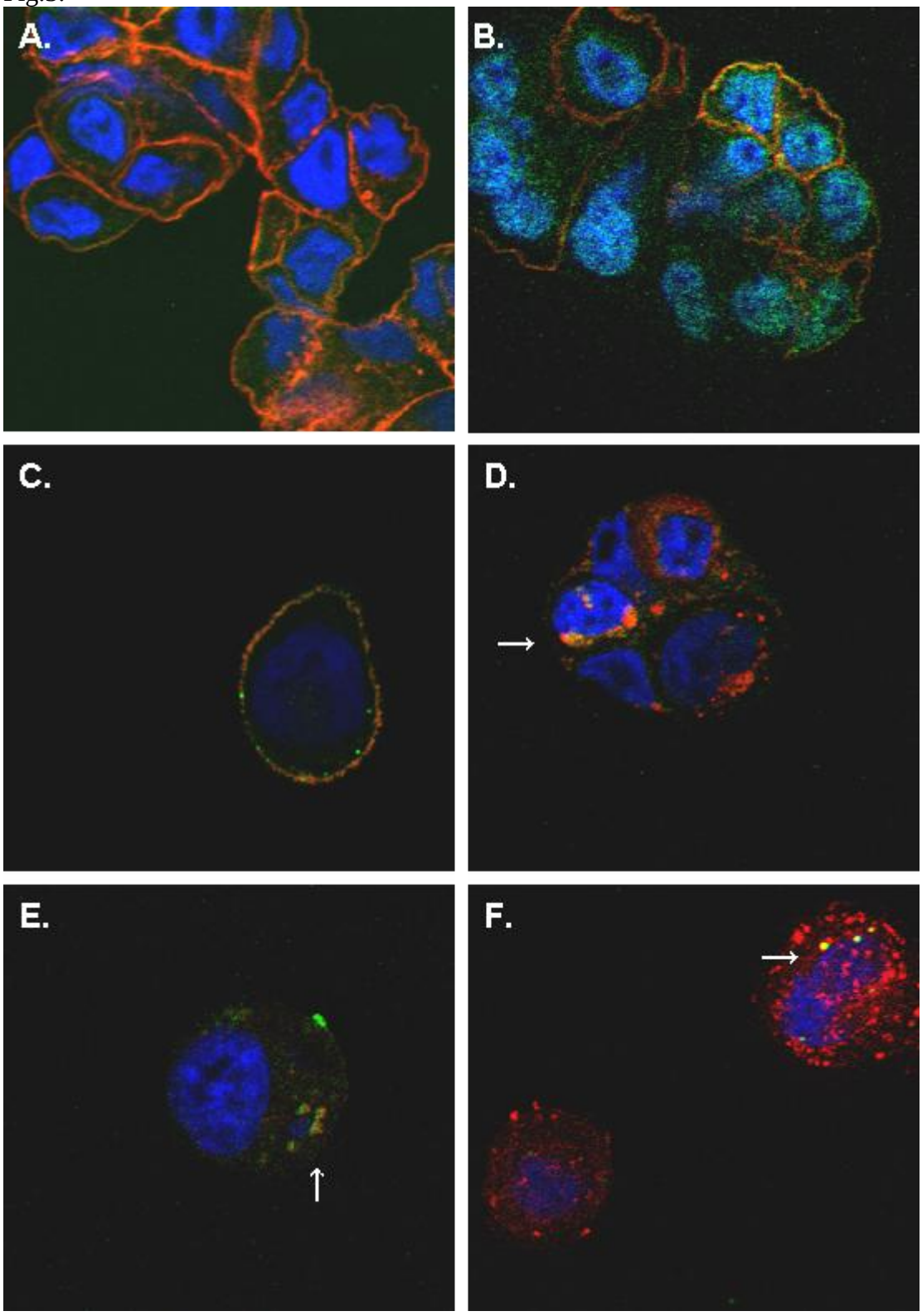

Fig.4.

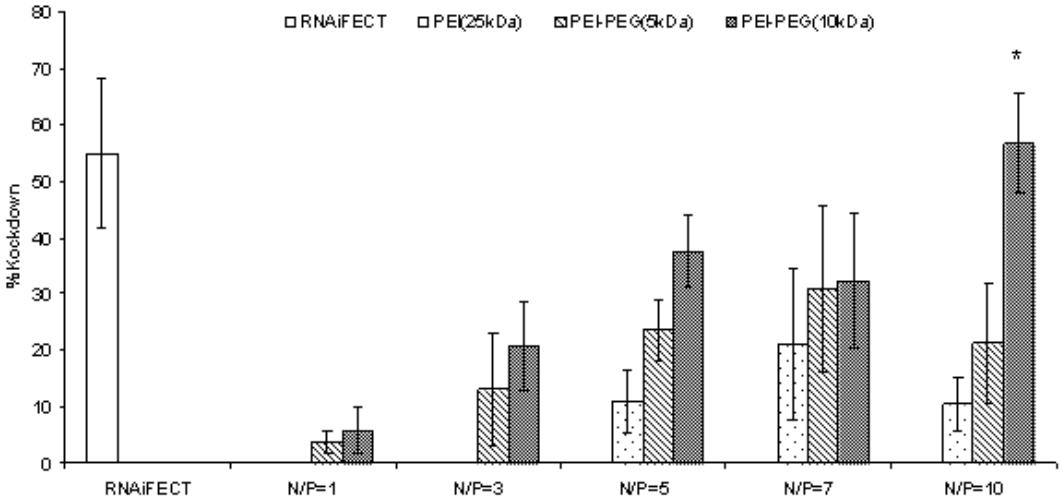
RNAiFECT
PEI(25kDa)
PEI-PEG(5kDa)
PEI-PEG(10kDa)
%Knockdown
80
70
60
50
40
30
20
10
0
*
RNAiFECT
N/P=1
N/P=3
N/P=5
N/P=7
N/P=10

Fig.5.

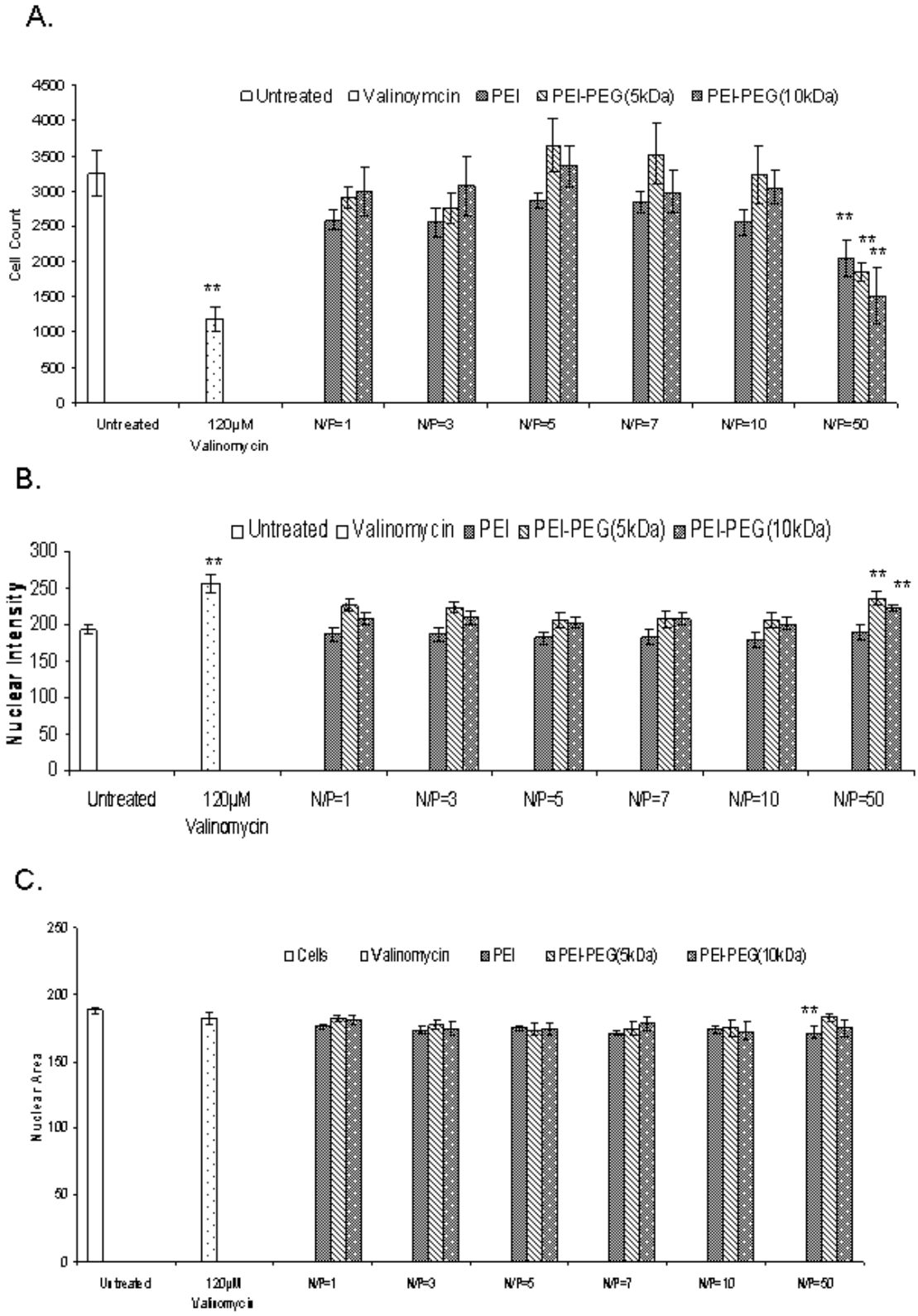
A.
Untreated
Valinoymcin
PEI
PEI-PEG(5kDa)
PEI-PEG(10kDa)
Cell Count
4500
4000
3500
3000
2500
2000
1500
1000
500
0
**
Untreated
120μM Valinomycin
N/P=1
N/P=3
N/P=5
N/P=7
N/P=10
N/P=50
B.
Untreated
Valinomycin
PEI
PEI-PEG(5kDa)
PEI-PEG(10kDa)
Nuclear Intensity
300
250
200
150
100
50
0
**
Untreated
120μM Valinomycin
N/P=1
N/P=3
N/P=5
N/P=7
N/P=10
N/P=50
C.
Cells
Valinomycin
PEI
PEI-PEG(5kDa)
PEI-PEG(10kDa)
Nuclear Area
250
200
150
100
50
0
**
Untreated
120μM Valinomycin
N/P=1
N/P=3
N/P=5
N/P=7
N/P=10
N/P=50

D.

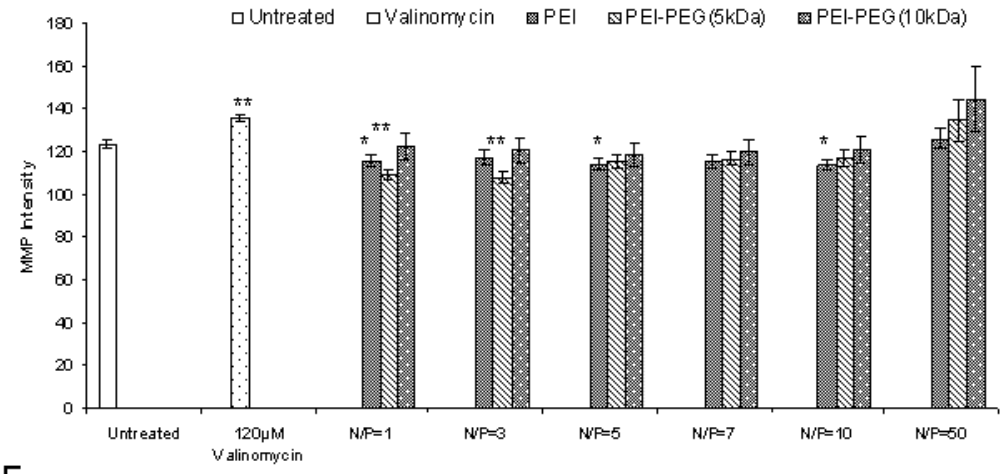
Untreated
Valinomycin
PEI
PEI-PEG(5kDa)
PEI-PEG(10kDa)
MMP Intensity
0
20
40
60
80
100
120
140
160
180
Untreated
120μM Valinomycin
N/P=1
N/P=3
N/P=5
N/P=7
N/P=10
N/P=50

E.

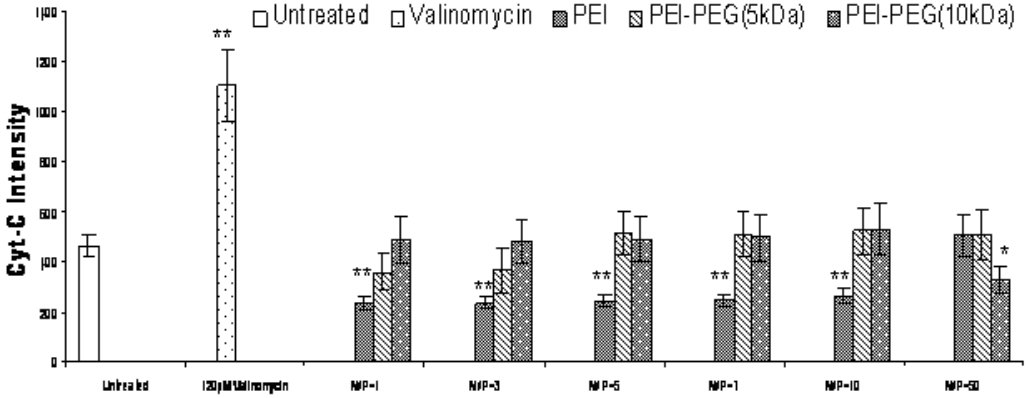
Untreated
Valinomycin
PEI
PEI-PEG(5kDa)
PEI-PEG(10kDa)
Cyt-C Intensity

F.

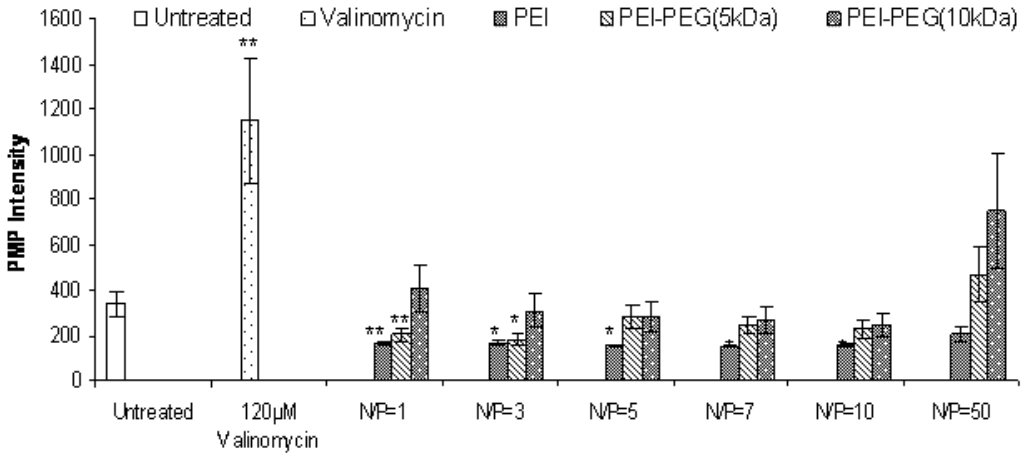
Untreated
Valinomycin
PEI
PEI-PEG(5kDa)
PEI-PEG(10kDa)
PMP Intensity
0
200
400
600
800
1000
1200
1400
1600
Untreated
120μM Valinomycin
N/P=1
N/P=3
N/P=5
N/P=7
N/P=10
N/P=50

Fig.6.

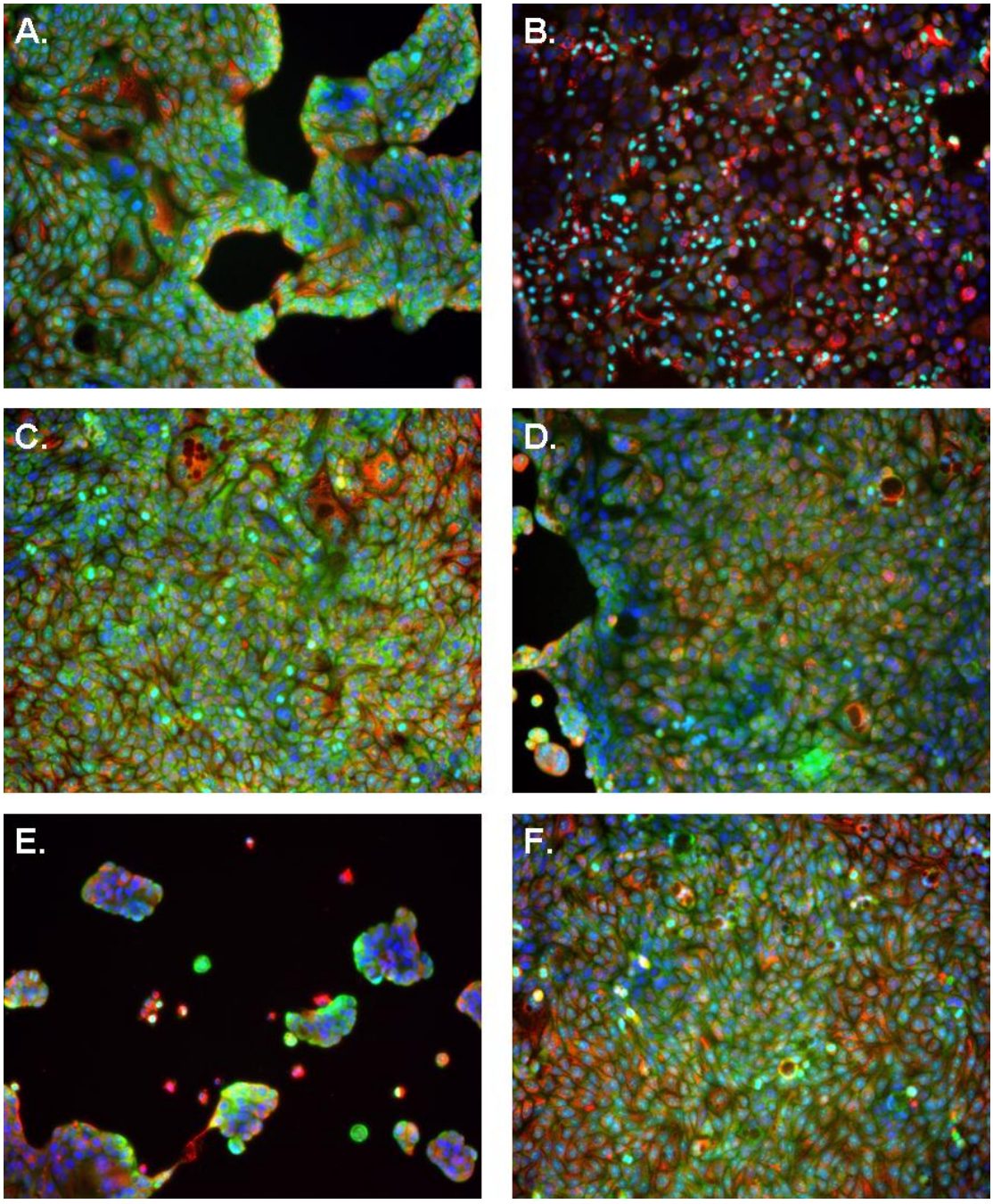

Fig.7.